JOURNAL OF CATALYSIS **167,** 550–559 (1997)
ARTICLE NO. CA971568

Propane Oxydehydrogenation over Molybdate-Based Catalysts

David L. Stern and Robert K. Grasselli[1]

Mobil Technology Company, Strategic Research Center, 600 Billingsport Road, Paulsboro, New Jersey 08066-0480

Received February 7, 1996; revised October 18, 1996; accepted December 4, 1996

Single and binary metal molybdates, supported on silica (80 wt% active phase/20 wt% SiO_2), having the formula $AMoO_4$, where A = Ni, Co, Mg, Mn, and/or Zn, and some ternary molybdates having the formula $Ni_{0.45}Co_{0.45}X_{0.066}MoO_4$, where X = P, Bi, Fe, Cr, V, and Ce, were investigated for the oxydehydrogenation of propane to propylene. The reaction is catalytic and is first order in propane disappearance, consistent with the abstraction of a methylene hydrogen being the rate limiting step. Propane conversion and yields of propylene produced vary greatly with the choice of the A metal of the molybdate and the surface area of the catalyst. At 560°C and atmospheric pressure, the highest propane conversion and highest propylene yields are obtained with $NiMoO_4/SiO_2$ (16% at 27% conversion), closely followed by $Ni_{0.5}Co_{0.5}MoO_4/SiO_2$. The molybdenum content of the compositions greatly influences the catalytic activity and useful product yields. The effect is largest for the Ni–molybdate system whose optimum lies at stoichiometry. The optimum activity of Co–molybdate lies at molybdenum lean compositions. Binary Ni–Co–molybdates are less sensitive to molybdenum level, offering a conveniently stable catalytic system for further mechanistic and technological optimization studies. Addition of redox elements V, Fe, Ce, and Cr enhances the activity of the Ni–Co–molybdates, with Cr addition holding most promise by retaining high selectivity at enhanced conversions and hence a possibility for desired lower process temperature operation. Our studies suggest, that the Ni–Co molybdate system provides an alternate to V-based catalysts for the activation of light paraffins. Futuristically, it holds promise as the paraffin activating component of a two component catalyst system for the direct conversion, in a single reactor, of propane to acrylic acid or acrylonitrile, with the second component being composed of one of the well known olefin converting, multicomponent mixed metal molybdates.

INTRODUCTION

The discovery and successful commercialization of heterogeneously catalyzed selective oxidations and ammoxidations of olefinic feedstocks to useful oxygen or nitrogen containing intermediates has had a major impact on both industrial and fundamental catalysis (1). More recently (2), research aims have shifted from functionalizing olefins to functionalizing the more abundant and less expensive paraffinic feedstocks, in an effort to meet future chemical, fiber, and polymer needs. One of the newer approaches has been selective oxydehydrogenation of lower alkanes, a two-electron oxidation, to functionalize paraffins to the corresponding olefins. The olefins produced may then be used as feedstocks in selective olefin oxidation and ammoxidation processes. Alternatively, paraffin activating catalysts may be combined with compatible olefin conversion catalysts to produce the corresponding oxygen or nitrogen containing unsaturated products directly.

In the area of paraffin oxydehydrogenation, several systems have emerged in recent years holding some promise for further study and development, particularly when applied to propane, *i*-butane, and *n*-butane. By far the most studied systems for propane upgrading center around vanadium (3), vanadium–antimony (4), vanadium–molybdenum (5), and vanadium–phosphorus based catalysts (6). Vanadium based systems activate propane at fairly low temperatures (down to 400°C), and it has been proposed that their effectiveness might stem from the "metalloradical character" of vanadium (7). Other alkane activating systems reported in the literature include metal phosphates (8), metal niobates (9), and metal molybdates (10–13).

Metal molybdates are particularly attractive since they exhibit, as do V-based systems, high activity for propane activation at relatively low temperature. While Hardman (10) studied primarily $CoMoO_4$ based catalysts for the oxydehydrogenation of propane to propylene, and Mazzochia *et al.* (11) primarily $NiMoO_4$, we undertook a broader investigation of propane oxydehydrogenation, studying single and binary molybdates of the formula $AMoO_4$, where A = Ni, Co, Mg, Mn, and/or Zn; some ternary molybdates of the formula $Ni_{0.45}Co_{0.45}X_{0.066}MoO_4$, where X = P, Bi, Fe, Cr, V, and Ce; and systems of the formula $Ni_{0.5}Co_{0.5}Y_{0.002}MoO_4$, where Y = K or Cs. A recent study of Moro-oka *et al.* (13) also examines propane oxidation with metal molybdate catalysts, and a review of propane oxydehydrogenation was recently reported by Cavani and Trifiro (14).

[1] Present address: Department of Chemical Engineering, University of Delaware, Newark, DE 19716-3116, and Department of Physical Chemistry, University of Munich, Sophienstrasse 11, D-80333 Munich, Germany.

0021-9517/97 $25.00

EXPERIMENTAL

The molybdate catalysts used in this study were prepared by refluxing aqueous solutions of stoichiometric amounts of the appropriate metal nitrate salts with ammonium heptamolybdate in the presence of silica sol (LUDOX AS-40). After drying the entire mixture and pulverizing, the resultant material was air calcined for 4 h at 290°C and 4 h at 600°C, pelletized, and sized to 20/40 mesh for catalytic evaluation. All catalysts were silica supported (80% active phase, 20% SiO_2).

The catalysts were characterized by powder diffraction techniques at room temperature, using relatively slow scan speeds (step size = 0.02°, scanning time = 2 s/step) with data accumulation from 4 to 70° 2θ. X-ray indexing was done by referencing to an internal standard of LaB_6 (NIST SRM 660). BET surface areas were measured with a Micromeritics ASAP 2400 N_2 physisorption apparatus.

The catalysts were evaluated in a fixed-bed, quartz microreactor, operated at ambient pressure. The gaseous feed to the reactor was prepared by metering propane, oxygen, and nitrogen with mass flow controllers. The reactor consisted of a wide bore top section (13 mm o.d., 10 mm i.d., 25 cm long) on top of a narrow bore exit line (6 mm o.d./ 2 mm i.d., 23 cm long). The pelletized, to 20/40 mesh sized, catalyst was mixed with an equal weight of 20/40 mesh acid washed quartz chips, the mixture then supported on quartz wool directly above the juncture in the reactor and covered with a 10-cm-long preheat zone of 20/40 mesh quartz chips to minimize dead volume. A 6-mm-o.d. quartz thermowell was centered axially in the reactor, which allowed for monitoring the temperature of the entire active catalyst bed. The catalyst bed was isothermal (±2°C), and the furnace temperature was adjusted for the exothermicity of the reaction in the catalyst bed. Temperatures reported herein are catalyst operating temperatures at conditions as specified.

The composition of the feed and product streams was determined by gas chromatography. The reactor effluent flowed directly through a heat traced line to a heated GC sampling valve to the GC (on-line analysis for oxygenates), then through an ice-cooled trap and a gas collection bulb to vent. Oxygenates and C_5^+ products were analyzed with a Varian GC using a 50-m DB-1 capillary column (FID detector). The gas collection bulb was sampled off-line with a Carle refinery gas analyzer (RGA) equipped with TCD and FID detectors. C_1, C_2°, $C_2^=$, and fixed gases (O_2, N_2, CO, and CO_2) were analyzed with the TCD, while saturated and unsaturated C_3 and C_4 components were analyzed on the FID. Water was not measured.

Catalysts were evaluated in two ways. In the first test, 1 g of 20/40 mesh catalyst dispersed in 1 g quartz chips was loaded in a reactor (see above), the catalyst was calcined under air (100 cc/min) for 1 h at 700°C, and feed (a 60 cc/min mixture of C_3°, O_2, and N_2 (15 : 15 : 70)) was introduced after cooling to 560°C under N_2 flush. The second test was performed in a likewise manner, except that feed was diverted as necessary to vary contact time (WHSV varied from 0.8 to 4, total gas flow rates of 250 to 30 cc/min), to obtain a range of hydrocarbon conversions.

Conversion is defined as the mole fraction of feed carbon or oxygen present in all reaction products. Yield is the mole fraction of feed carbon present in a product, and selectivity is yield divided by conversion. The data reported here were obtained at oxygen conversions of 80% or less. The background reactivity of both propane and propylene with oxygen, measured in a reactor filled with quartz chips, is insignificant (less than 1.5% under the most severe conditions studied). Carbon and hydrogen closures were typically better than 97%, oxygen closures typically better than 95% (closures were calculated based on reaction stoichiometry, including the anticipated water formation). The results reported are corrected for any carbon nonclosure.

RESULTS AND DISCUSSION

Catalyst Characterization

The X-ray powder diffraction patterns of the metal molybdates $AMoO_4$, where A = Ni, Co, Mg, Mn, and Zn, are shown in Fig. 1. As reported in the literature (15–17), three structural types are possible for these molybdates: α-$MnMoO_4$, α-$CoMoO_4$, and $NiWO_4$ (α-$ZnMoO_4$). The patterns for cobalt, magnesium, and manganese molybdate reference well to the α-$MnMoO_4$ structural type, while those for nickel molybdate reference to the α-$CoMoO_4$ structural type. The two structural types are similar, containing octahedrally coordinated cations (Ni^{2+}, Co^{2+}, Mg^{2+}, Mn^{2+}), but either tetrahedrally (α-$MnMoO_4$) or octahedrally coordinated (α-$CoMoO_4$) molybdenum. As reported by Sleight and Chamberlain (17), the structures of some of these materials interconvert on heating, while others

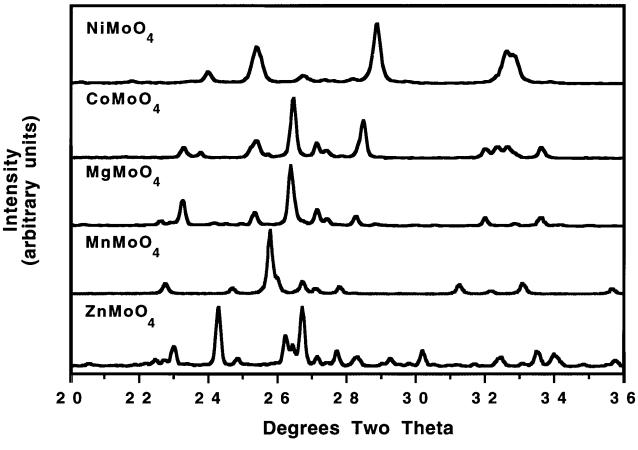

FIG. 1. XRD of metal molybdates ($AMoO_4$).

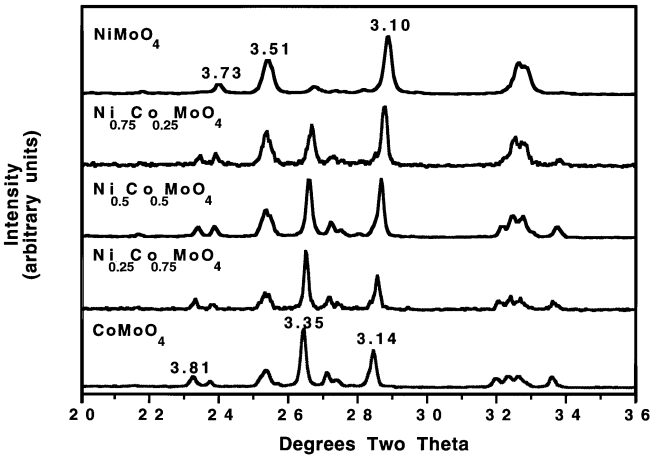

FIG. 2. XRD of binary metal molybdates ($Ni_{1-x}Co_xMoO_4$).

do not. Thus, reversible interconversion of $CoMoO_4$ from the α-$CoMoO_4$ structure type to the α-$MnMoO_4$ structure type occurs at 500°C, while such interconversion occurs for $NiMoO_4$ at or above 690°C. The $MgMoO_4$ and $MnMoO_4$ systems do not interconvert upon heating and retain their α-$MnMoO_4$ structure type throughout the temperature range studied. Our zinc molybdate references well to the $NiWO_4$ structural type. This structural type is formed for the other molybdates evaluated here only under high pressure synthesis conditions (15, 16) and is thus unimportant in our current study.

A series of binary nickel cobalt molybdates was also prepared ($Ni_{1-x}Co_xMoO_4$, where $x = 0$, 0.25, 0.5, 0.75, and 1). The X-ray diffraction patterns are presented in Fig. 2. As discussed above, the XRD patterns of nickel and cobalt molybdate are illustrative of the patterns for the α-$CoMoO_4$ and α-$MnMoO_4$ structural types, with characteristic d-spacings centered at 3.73, 3.51, and 3.09 Å and at 3.81, 3.35, and 3.14 Å for these two phases, respectively. The (2 2 0) reflection (ca. 28.5° 2θ) is common to both structural types and a lattice expansion is observed for the series $Ni_{1-x}Co_xMoO_4$, going from $NiMoO_4$ to $CoMoO_4$, by following the shift in the d-spacing of the (2 2 0) reflection from 3.096 to 3.140 Å, respectively. This increase in d-spacing is consistent with the increase in six coordinate ionic radii of Ni^{2+} (0.69 Å) to Co^{2+} (0.74 Å) and is reflected in a linear increase across the entire series with an increase in the Co/Ni ratio (Fig. 3). Since both the cell dimensions and the relative intensities representative of these two compounds vary linearly with the Ni/Co atomic ratio, and by considering the size and gross chemical nature of Ni^{2+} and Co^{2+} ions, application of Vegard's Law (19) leads us to conclude that the structures of the mixed nickel–cobalt–molybdates are solid solutions of $NiMoO_4$ and $CoMoO_4$ in a common molybdate lattice.

X-ray diffraction patterns of binary $Ni_{0.5}A_{0.5}MoO_4$, where A = Co, Mg, Mn, and Zn reveal that introduction of any one of these four metals greatly influences the structural behavior of the Ni–molybdate host. All four metals

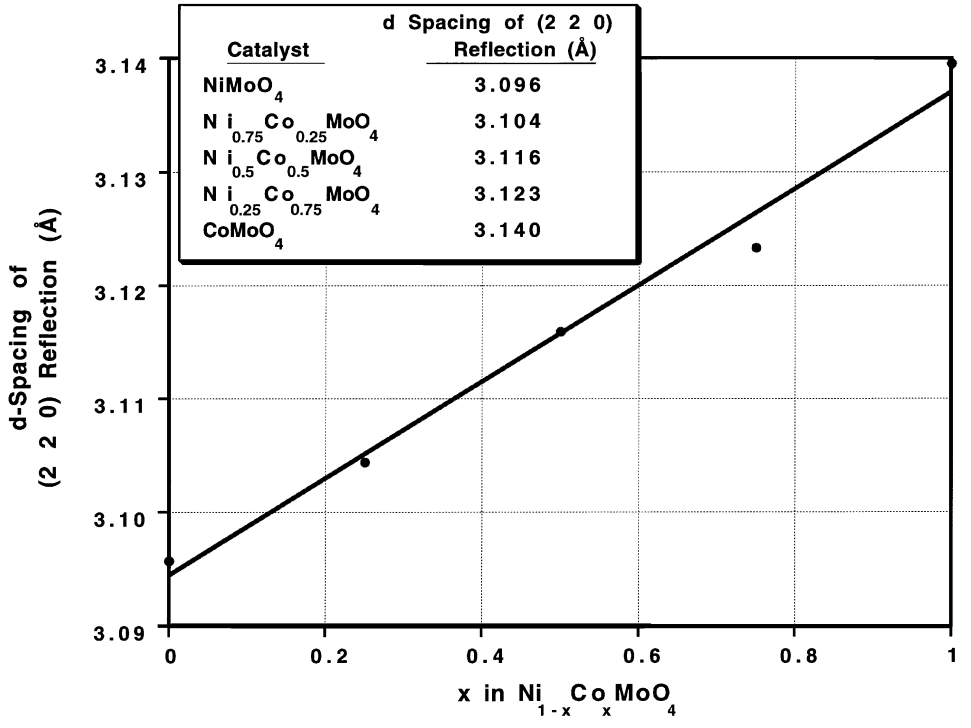

FIG. 3. Lattice expansion of $Ni_{1-x}Co_xMoO_4$ with increasing Co content.

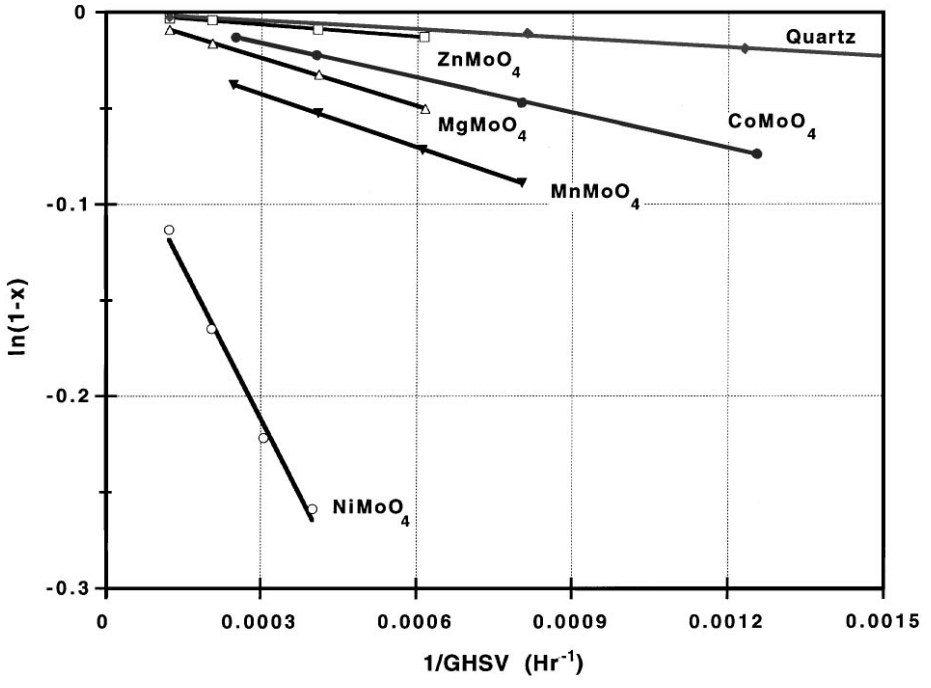

FIG. 4. First order kinetic plot for propane oxidation over metal molybdates.

shift the structure of the base from the α-Co–molybdate type (octahedral Mo coordination) to the α-Mn–molybdate type (tetrahedral Mo coordination). X-ray diffraction patterns of substituted Ni–Co–molybdates were also taken ($Ni_{0.45}Co_{0.45}X_{0.066}MoO_4$, where X = P, Fe, Bi, Ce, Cr, and V, and $Ni_{0.5}Co_{0.05}Y_{0.002}MoO_4$, where Y = K, Cs). The X-ray patterns of these substituted compounds are similar to that of the base $Ni_{0.5}Co_{0.5}MoO_4$, leading us to conclude that introduction of low levels of auxiliary metals into the Ni–Co–molybdate host does not alter significantly the structure of the host.

Catalyst Evaluation

A. $AMoO_4$, where A = Ni, Co, Mg, Mn, Zn. The disappearance of propane over this set of catalysts is first order as revealed by the straight lines in plotting the logarithm of (1-propane conversion) vs inverse space velocity (Fig. 4). This observation is consistent with C–H bond breaking of a methylene hydrogen being the rate limiting step in the activation of propane.

The activity varies greatly with the choice of the *A* metal and the surface area of the catalyst (Table 1):

Relative activity:	Ni ≫	Mn >	Mg >	Co >	Zn >	Quartz
Relative *k*'s:	100	18	16	12	4	3
Relative surface area normalized *k*'s:	100	50	29	21	12	1

While the surface area has a large effect on the conversion of propane, the activation of propane is more strongly

TABLE 1

Summary of Catalytic Data for Propane Oxidation over Metal Molybdates

Catalyst	Surface area (m^2/g)	Selectivity to useful products at 7% C_3° conversion	Selectivity to useful products at 15% C_3° conversion	k ($s^{-1} \times 10^{-3}$)	k/SA
$NiMoO_4$	39	85.2	66.2	146	3.74
$CoMoO_4$	22	64.0	46.4	17	0.77
$MnMoO_4$	14	65.5	48.2	26	1.86
$MgMoO_4$	21	80.2	63.0	23	1.09
$ZnMoO_4$	13	64.8	32.5	6	0.46
$Ni_{0.75}Co_{0.25}MoO_4$	33	86.2	71.9	83	2.52
$Ni_{0.5}Co_{0.5}MoO_4$	33	86.3	71.5	52	1.58
$Ni_{0.25}Co_{0.75}MoO_4$	24	67.2	49.7	13	0.54
$Ni_{0.5}Mn_{0.5}MoO_4$	20	79.0	58.1	46	2.30
$Ni_{0.5}Mg_{0.5}MoO_4$	20	82.7	62.5	30	1.50
$Ni_{0.5}Zn_{0.5}MoO_4$	15	74.9	44.1	12	0.80
$Ni_{0.45}Co_{0.45}P_{0.066}MoO_4$	19	85.3	65.5	31	1.63
$Ni_{0.45}Co_{0.45}Fe_{0.066}MoO_4$	22	67.5	49.5	94	4.27
$Ni_{0.45}Co_{0.45}Bi_{0.066}MoO_4$	22	29.4	—	11	0.50
$Ni_{0.45}Co_{0.45}Ce_{0.066}MoO_4$	22	76.7	63.5	99	4.50
$Ni_{0.45}Co_{0.45}Cr_{0.066}MoO_4$	23	85.0	70.5	94	4.09
$Ni_{0.45}Co_{0.45}V_{0.066}MoO_4$	12	55.5	41.4	187	15.6
$Ni_{0.5}Co_{0.5}K_{0.002}MoO_4$	24	71.4	59.1	28	1.17
$Ni_{0.5}Co_{0.5}Cs_{0.002}MoO_4$	22	69.4	—	10	0.45
Quartz-packed reactor	—	—	—	4	—

Note. Conditions: $C_3^\circ/O_2/N_2$ feed (15/15/70 feed ratio), WHSV varied to achieve a wide range of C_3° conversions, 560°C, 1 atm total pressure.

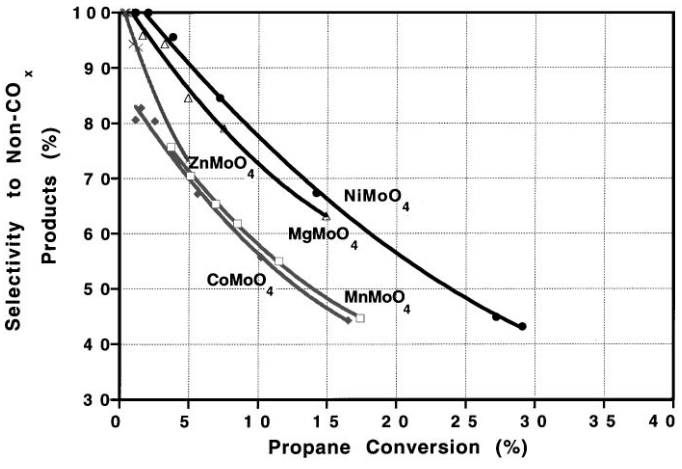

FIG. 5. Propane oxidation over metal molybdates (AMoO$_4$).

influenced by the nature of the *A* metal. Most probably it is the nature of the molybdenum oxygen bond, as influenced by the nature of the adjacent *A* metal, which is responsible for the activation of propane. Thus, a Ni–O–Mo–O is much more active than a Zn–O–Mo–O.

The selectivity of non-CO_x products (i.e., mainly propylene) decreases with propane conversion (Fig. 5), implying consecutive reaction and destruction of the propylene intermediate as the concentration of propylene builds up. In most cases the non-CO_x (i.e., useful) products consist of about 96% propylene, 3–5% acrolein, and 0–1% acrylic acid. The selectivity at comparable conversion is highest for the $NiMoO_4$ catalyst, followed closely by $MgMoO_4$. The systems $CoMoO_4$, $MnMoO_4$, and $ZnMoO_4$ form a catalyst set of lower selectivity.

It is apparent from these results (i.e., activity being strongly influenced by the *A* metal of the molybdate) that propane activation and its conversion to propylene is a surface catalyzed reaction and not a homogeneous phase, radical generated reaction.

B. $Ni_{0.5}A_{0.5}MoO_4$, where A = Co, Mg, Mn, Zn. Binary metal molybdates containing nickel as one of the metals do not exhibit any activity synergism over and above the base reactivity of $NiMoO_4$ itself (Fig. 6). However, there appears to be some synergy between Ni and Co in the binary system $Ni_{0.5}Co_{0.5}MoO_4$. By comparing the results of the simple metal molybdates (Fig. 4) with those of the binary metal molybdates (Fig. 6), it is apparent that the Ni–Co system is the most active of the binary systems studied, even though $CoMoO_4$ ranked fourth among the simple molybdates. The activity ranking of the binaries is: $Ni_{0.5}Co_{0.5}MoO_4 > Ni_{0.5}Mn_{0.5}MoO_4 > Ni_{0.5}Mg_{0.5}MoO_4 > Ni_{0.5}Zn_{0.5}MoO_4$.

Similarly, among the binary molybdates, the selectivity to non-CO_x products (primarily propylene) is highest at comparable conversions (numbers in parentheses are selectivities at 7 and 15% propane conversions, respectively) for the $Ni_{0.5}Co_{0.5}MoO_4$ (86, 72), followed by Ni/Mg (83, 63), Ni/Mn (79, 58), and Ni/Zn (75, 44) molybdates (Table 1). At these conversion levels the selectivity to non-CO_x products of the binary molybdate $Ni_{0.5}Co_{0.5}MoO_4$, and the most active

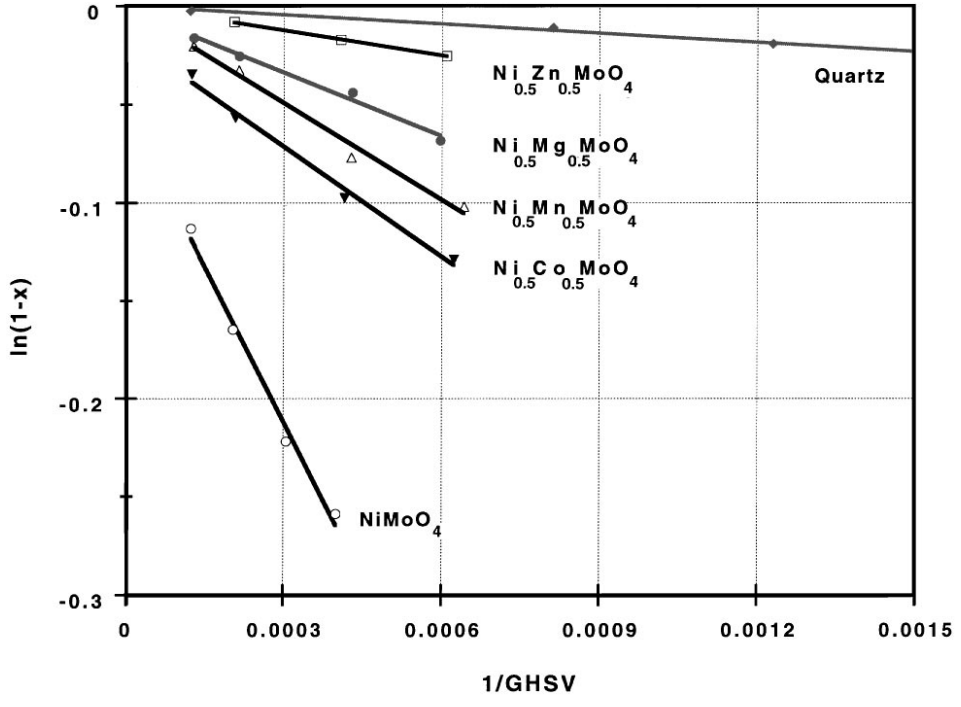

FIG. 6. First order kinetic plot for propane oxidation over binary metal molybdates ($Ni_{0.5}M_{0.5}MoO_4$).

simple molybdate $NiMoO_4$ (85, 66) are comparable. These observations, in conjunction with the observation that binary molybdates are synthetically easier to reproduce than the catalytically most active simple molybdate $NiMoO_4$, led us to investigate the binary Ni–Co–molybdate system more thoroughly.

C. $Ni_{1-x}Co_xMoO_4$, where $x = 0$ to 1. The disappearance of propane is also first order for the Ni/Co binary molybdates, as evidenced by the straight lines obtained when plotting the logarithm of (1-propane conversion) against inverse space velocity. The activity ranking and relative surface areas (Table 1) are:

Relative activity:	$Ni_1 \sim Ni_{0.75}Co_{0.25} > Ni_{0.5}Co_{0.5} > Ni_{0.25}Co_{0.75} \sim Co_1$				
Relative k's:	100	87	42	11	15
Relative surface area normalized k's:	100	90	78	60	45

A plot (Fig. 7) of k vs the Ni/Co concentration gives an S shape curve which tracks approximately the surface area of the respective catalysts. The S shape curve suggests also that replacement of up to 25% of either Ni by Co or Co by Ni is catalytically, as well as surface-area-wise, mainly dominated by the nature of the respective majority metal on either end of the compositional range.

A similar trend is also seen with the non-CO_x selectivity as a function of propane conversion (Fig. 8). At comparable conversion, the high Ni containing catalysts form one set of curves while the high Co containing catalysts form a second set of curves. The non-CO_x yield is higher for the high Ni compositions than for the high Co compositions.

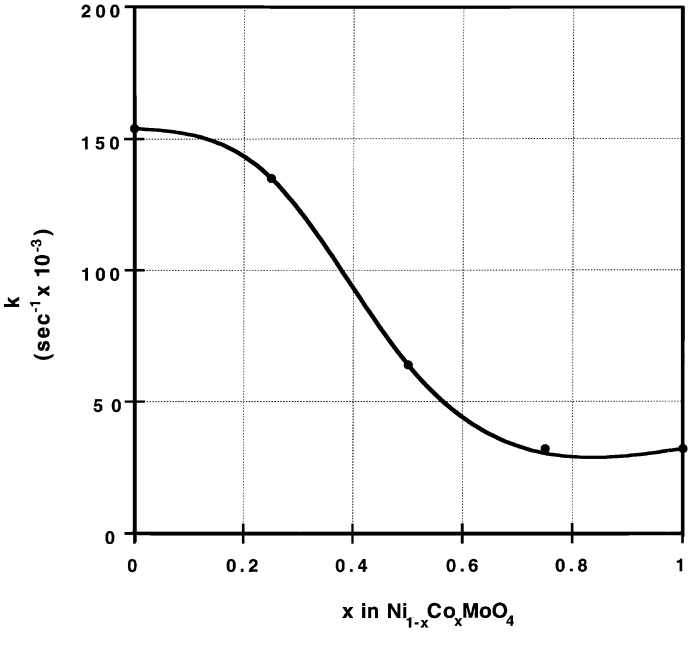

FIG. 7. First order rate constant (k) vs cobalt content in $Ni_{1-x}Co_xMoO_4$.

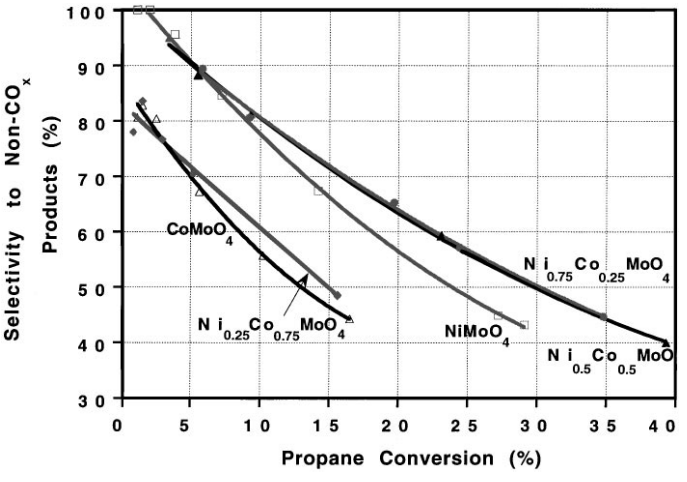

FIG. 8. Selectivity to non-CO_x products vs propane conversion as a function of Ni/Co ratio.

D. A $Mo_{1\pm x}O_y$, where $A =$ Ni, Co and $x = 0$ to 0.1. A study of the A/Mo ratio (Table 2, Fig. 9) reveals that both the catalytic activity and the non-CO_x yield are highly sensitive to the molybdenum content of these compositions. Particularly sensitive is the Ni composition, where the stoichiometric composition $NiMoO_4$ exhibits by far the highest propane activity, as well as the highest non-CO_x yield. Both fall off precipitously on either side of stoichiometry (on the molybdenum rich, as well as, the molybdenum lean side).

Co–molybdate compositions are much less sensitive to the molybdenum content. Unlike the Ni compositions, the optimum activity and non-CO_x yield are not attained at Co/Mo stoichiometry, but rather at molybdenum lean compositions. Since $CoMoO_4$ is a well known catalyst for converting propylene to acrolein, it is possible that the stoichiometric compound or a molybdenum rich composition thereof provides for facile adsorption of propylene, the first formed product of propane conversion, forming acrolein, which readily converts further to CO_x under the conditions used in the study. In addition, the chemisorbed propylene and acrolein can inhibit the interaction of the propane with the surface, resulting in self-poisoning of the surface and hence lower rates of propane activation. These issues, including a comprehensive analysis of propane activation kinetics over these molybdates, are discussed in a subsequent article in this journal (20).

The $Ni_{0.5}Co_{0.5}Mo_{1\pm x}O_y$ compositions lie between the extremes of $NiMo_{1\pm x}O_y$ and $CoMo_{1\pm x}O_y$, with regard to the variation in propane conversion and propylene yield as a function of Mo content. They are significantly less affected than the Ni only composition and somewhat more affected than the Co only composition. It is a good compromise composition for further studies (20).

TABLE 2

Summary of Catalytic Data for Propane Oxidation over Metal Molybdate Catalysts

Catalyst	C_3° conversion	Non-CO_x selectivity	Yield	$C_3^=$ selectivity	Acrolein selectivity	Surface area	O_2 conversion	k ($sec^{-1} \times 10^{-3}$)	k/SA
$Ni_{1.1}MoO_x$	14.8	68.5	10.1	63.8	4.6	39	26.1	80	2.05
$NiMoO_4$	26.6	64.0	17.0	60.4	3.6	40	60.8	154	3.85
$NiMo_{1.1}O_x$	4.0	85.0	3.4	80.7	4.4	31	4.6	20	0.65
$Ni_{0.75}Co_{0.25}MoO_4$	23.7	64.3	15.2	60.2	4.1	36	47.3	135	3.75
$Ni_{0.55}Co_{0.55}MoO_x$	10.9	68.2	7.4	64.3	3.9	33	21.9	58	1.76
$Ni_{0.5}Co_{0.5}MoO_4$	12.1	75.8	9.2	71.4	4.4	31	20.3	64	2.06
$Ni_{0.5}Co_{0.5}Mo_{1.1}O_x$	4.5	82.4	3.7	77.4	5.1	24	6.0	23	0.96
$Ni_{0.25}Co_{0.75}MoO_4$	3.4	80.0	2.7	75.8	4.2	24	6.7	17	0.71
$Co_{1.1}MoO_x$	6.6	66.2	4.4	63.6	2.6	24	6.6	34	1.42
$CoMoO_4$	4.4	70.0	3.1	65.4	4.6	18	8.4	23	1.28
$CoMo_{1.1}O_x$	2.7	86.8	2.3	82.7	4.1	20	5.3	14	0.70
$MgMoO_4$	5.1	81.9	4.2	77.5	4.5	21	7.6	26	1.24
$MnMoO_4$	6.2	68.6	4.3	64.3	4.3	14	13.4	32	2.29
$ZnMoO_4$	1.4	93.8	1.3	90.7	3.2	13	3.0	7	0.54

Note. Conditions: 560°C, 1 atm. Feed (in cc/min): 9 C_3°/9 O_2/42 N_2 over 1 g catalyst.

A plot of k vs surface area (Fig. 10) for stoichiometric, molybdenum lean, and molybdenum rich compositions reveals that as a group, stoichiometric molybdates are the most active, the molybdenum lean molybdates less active, and the molybdenum rich compositions the least active. It is interesting to note that the activity of the stoichiometric molybdates rises approximately with the cube of the surface area, the molybdenum-lean compositions with the square, and the molybdenum-rich molybdates linearly with surface area. The exact meaning of this behavior is unclear at this time. However, it is clear that propane oxydehydrogenation is a surface catalyzed reaction, and not a gas phase, free radical initiated reaction, otherwise such large surface area dependencies would not be found. And since for these and other reasons discussed above, the activation of propane is a surface catalyzed reaction, and since all of our studies point to the active sites being composed of *A*–O–Mo–O moieties, it is safe to assume that the largest concentration of such moieties will be found on the surface with stoichiometric compositions. Furthermore, the nature of the *A* metal in

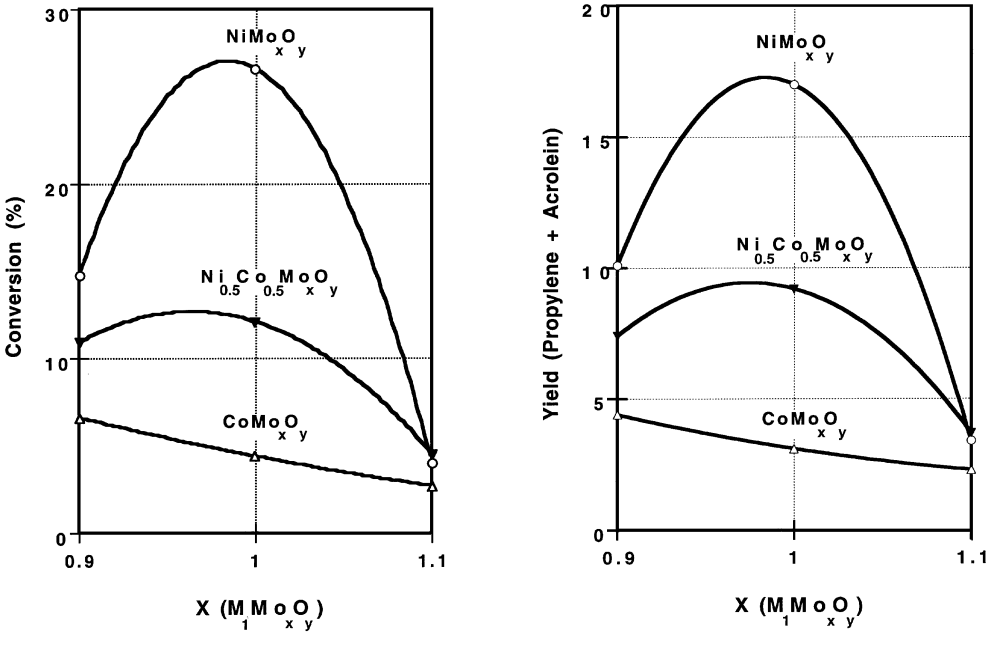

FIG. 9. Conversion and non-CO_x yield as a function of the molybdenum content in nickel, cobalt, and nickel–cobalt molybdates.

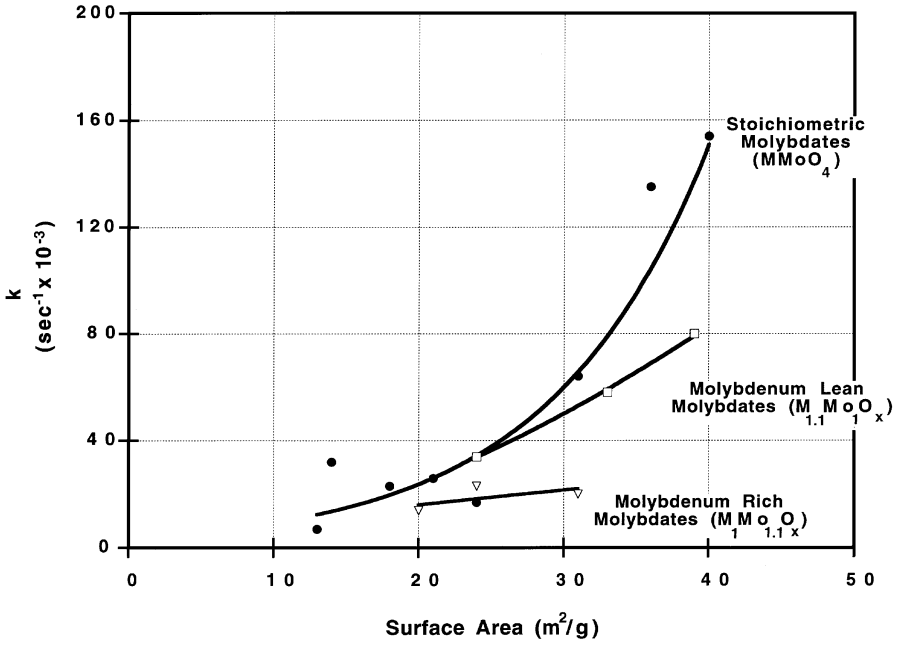

FIG. 10. First order rate constant (k) vs surface area of stoichiometric, molybdenum-lean, and molybdenum-rich metal molybdates.

the A–O–Mo–O catalytic site is of uppermost importance for the activation of the paraffin, with Ni being the most efficient A metal of those studied. Thus, Ni-rich compositions lie in activity above the Co-rich compositions. Since, according to our studies the oxygen of the Mo adjacent to the A metal in the A–O–Mo–O site is the actual abstractor of the rate limiting methylene hydrogen from the propane, molybdenum lean compositions will be less active than the stoichiometric ones (square dependence with surface area for the former and a cube dependence for the latter). Finally, it can be reasoned that the molybdenum rich compositions will be the least active among the studied molybdates (linear dependence of activity with surface area), because the concentration of A–O–Mo–O sites on the surface will be the lowest. As the concentration of molybdenum increases, the amount of suprasurface MoO_3 can become significant (up to a monolayer) and ultimately excessive (greater than a monolayer), with the result, that the catalyst begins to act as if it were simply MoO_3 supported on $AMoO_4$; it becomes relatively inactive.

The selectivity to non-CO_x products at comparable propane conversion (Tables 1 and 2) is highest for the Mo-rich and lowest for the Mo-lean compositions. A possible explanation consistent with the activity results of these catalysts is that the Mo-lean compositions possess a high A metal surface concentration which can lead to the formation of surface A–O–A moieties and higher A–O–A clusters and ultimately to the formation of surface AO (e.g., NiO). Either of these possibilities would lead to high, nonselective propane conversions, resulting in waste products. Therefore, the surface of A-rich compositions attacks and combusts the formed propylene more readily than the surface of the stoichiometric or Mo-rich compositions. Among this series, the Mo-rich compositions are the most selective ones in forming non-CO_x products (i.e., propylene), implying that consecutive combustion of the first formed propylene and the second formed acrolein is less prevalent here than with compositions having less molybdenum. This is certainly consistent with the site isolation theory of selective oxidation catalysis (21), and the behavior of multicomponent catalysts containing excess molybdenum for the selective oxidation or ammoxidation of olefins to the corresponding aldehydes, acids, or nitriles (22).

E. Promoted $Ni_{0.5}Co_{0.5}MoO_x$ catalysts. A brief study of some promoted compositions (i.e., $Ni_{0.45}Co_{0.45}X_{0.066}MoO_4$, where $X =$ P, Fe, Bi, Ce, Cr, and V, and $Ni_{0.5}Co_{0.5}Y_{0.002}MoO_4$, where $Y =$ K or Cs (Table 1)) reveals that the activity of the modified catalysts varies greatly with the addition of small amounts of dopants:

Modifier:	V	≫	Ce	~	Fe	~	Cr	>	Base	>	P	~	K	>	Bi	~	Cs
Relative k's:	100		53		50		50		27		17		15		6		5
Relative surface area normalized k's:	100		29		27		26		10		10		8		3		3

The addition of redox elements greatly enhances catalytic activity, e.g., V by a factor of 4 (absolute), 10 (relative); Ce, Fe, Cr, by a factor of 2 (absolute), 3 (relative). Addition of P is innocuous, while the addition of Bi, as well as,

alkalis (K, Cs) greatly decreases the catalytic activity of the base.

Likely explanations for the observed behavior are that the addition of elements capable of one-electron redox shuttle increase the catalytic activity of the base molybdate by keeping the latter in a high, and therefore active, oxidation state (i.e., Mo^{6+}). Conversely, addition of alkalis reduces the effectiveness of the redox shuttle, decreasing the activity of the base. Addition of Bi, through the likely formation of some $Bi_xMo_yO_z$, provides for ready oxygen insertion into the first formed propylene product, leading to acrolein whose strongly inhibited desorption leads to blockage of propane adsorption sites (i.e., decreased activity) and ready formation of CO_x (i.e., decreased non-CO_x selectivity).

While the addition of redox elements V, Ce, Fe, and Cr leads to lower propylene (non-CO_x product) selectivities at the reaction temperature (560°C) studied (exception is Cr), their markedly higher activities provide for the technologically important possibility of carrying out the reaction at lower temperatures, which is not incumbent upon the base itself. Therefore, it is surmised that higher propylene yields at comparable conversions would be obtained at lower temperatures with redox promoted systems. Of particular promise is Cr, followed by Ce and Fe promoted systems. Additional work is needed to work out the compositional details.

CONCLUSIONS

A brief study of propane oxydehydrogenation to propylene over first row, divalent metal molybdates ($AMoO_4$) supported on SiO_2 reveals that the reaction is catalytic and not a gas phase radical initiated reaction. It further reveals that the reaction is first order in propane, consistent with the rate limiting step being the C–H bond breaking abstraction of a methylene hydrogen from the propane molecule.

The yields of propylene at constant conversion vary greatly between the catalysts studied, and the highest observed yields (16% at 26.6% conversion) are obtained with $NiMoO_4$ and $Ni_{0.5}Co_{0.5}MoO_4$. The $NiMoO_4$ system is very sensitive to the Ni/Mo ratio and performs best at stoichiometry. Conversely, $CoMoO_4$ gives the highest propylene yields with a molybdenum lean composition. $Ni_{1-x}Co_xMoO_y$ compositions give results intermediate to the two end members, with up to about 25% of the alternate elements incorporation giving approximately the behavior of the respective end members. To achieve stability and ease of catalyst reproducibility, Ni–Co–molybdates are preferred over single element molybdates. Propane activation kinetics and its reaction network over $Ni_{0.5}Co_{0.5}MoO_4$ are reported in another publication (20).

Incorporation of redox elements such as V, Ce, Fe, and Cr greatly increases the activity of the base: e.g., V by a factor of four; Ce, Fe, and Cr by a factor of two. This allows for propane activation and possible process operation at lower temperatures (i.e., below 560°C), concomitant with anticipated improved useful product yields. Of particular promise is the Cr promoted system.

We conclude further that the Ni–Co–molybdate systems are at least as effective as V-based catalysts for the activation of propane to propylene. Unfortunately, the rapid oxidation of the first formed propylene to subsequent products (such as acrolein and CO_x) limits the usefulness of these systems for the production of propylene from propane at high conversions. Operation at low propane conversions results in good propylene selectivities; however, that would require high recycle of unconverted propane, which is impractical. Another process possibility is operation at high propane to oxygen ratio, but that also requires high propane recycle. Cyclic (redox) mode of operation in absence of gaseous oxygen holds some promise, as do redox element promoted (e.g., Cr containing) systems. Both need further study.

A possible future application of the Ni–Co–molybdate system, particularly a redox promoted one, might be in the conversion of propane in the presence of NH_3 and oxygen (air) to acrylonitrile. The idea (22) is to combine the paraffin activating Ni–Co–molybdate catalyst with one of the well known multicomponent mixed metal molybdates (23) in a single reactor, converting the propylene intermediate formed *in situ* to acrylonitrile. Well dispersed physical or compacted mixtures of these two types of catalysts may achieve this goal. It is necessary to temperature match the two catalysts, i.e., to find a common compromise temperature optimum by compositionally tuning both of these compositions. Either the Ni–Co–molybdate must be modified to operate at a lower temperature by addition of redox elements such as V, Fe, Ce, Cr (see above), or the multicomponent molybdate catalyst (23) must be modified to operate at higher temperature by adjusting its redox behavior (e.g., replacing Fe by Ce).

ACKNOWLEDGMENT

The authors acknowledge Lorenzo DeCaul for carrying out a large number of the catalyst evaluations reported in this study.

REFERENCES

1. Grasselli, R. K., *J. Chem. Ed.* **63**, 216 (1986).
2. Grasselli, R. K., and Burrington, J. D., *Adv. Catal.* **30**, 133 (1981).
3. (a) Kung, M. C., and Kung, H. H., *J. Catal.* **134**, 668 (1992); (b) Corma, A., Lopez Nieto, J. M., and Paredes, N., *J. Catal.* **144**, 425 (1993).
4. (a) Guttmann, A. T., Grasselli, R. K., and Brazdil, J. F., US Patent 4,746,641 (1988); (b) Cavani, F., Centi, G., Trifiro, F., and Grasselli, R. K., *Catal. Today* **3**, 185 (1988); (c) Catani, R., Centi, G., Trifiro, F., and Grasselli, R. K., *Ind. Eng. Chem. Res.* **31**, 107 (1992); (d) Andersson, A., Andersson, S. L. T., Centi, G., Grasselli, R. K., Sanati, M., and Trifiro, F., "Proceedings, 10th International, Congress on Catalysis, Budapest, 1992" (L. Guczi, F. Solymosi, and P. Tetenyi, Eds.). Akadémiai kiadó, Budapest, 1993; (e) Andersson, A.,

Andersson, S. L. T., Centi, G., Grasselli, R. K., Santi, M., and Trifiro, F., *Appl. Catal. A* **113**, 43 (1994).
5. (a) Kim, Y.-C., Ueda, W., and Moro-oka, Y., *Catal. Today* **13**, 673 (1992); (b) Oshima, K., Kayo, A., Umezawa, T., Kiyono, K., and Sawaki, I., European Patent 529,853 (1992); (c) Bartek, J. P., Ebner, A. M., and Brazdil, J. F., US Patent 5,198,580 (1993).
6. (a) Ai, M., *Catal. Today* **12**, 679 (1992); (b) Ai, M., *J. Catal.* **101**, 389 (1986).
7. Grasselli, R. K., "Surf. Prop. Catal. Non-Metals" (J. Bonelle, B. Delmon, and E. Derouane, Eds.), p. 273. Reidel, Dordrecht, 1983.
8. (a) Takita, Y., Yamashita, H., and Moritaka, K., *Chem. Lett.*, 1733 (1989); (b) Honda, T., and Terada, K., European Patent 428,413 (1990).
9. Smits, R. H. H., Seshan, K., and Ross, J. R. H., *ACS Prepr. Div. Petr. Chem.* **37**, 1121 (1992).
10. (a) Hardman, H. F., US Patent 4,131,631 (1978); (b) Hardman, H. F., US Patent 4,255,284 (1981).
11. (a) Mazzocchia, C., Tempesti, E., and Aboumrad, C., US Patent 5,086,032 (1992); (b) Mazzocchia, C., Aboumrad, C., Diagne, C., Tempesti, E., Herrmann, J. M., and Thomas, G., *Catal. Lett.* **10**, 181 (1991).
12. (a) Suresh, D. D., Seeley, M. J., Nappier, J. R., and Friedrich, M. S., US Patent 5,171,876 (1992); (b) Seeley, M. J., Friedrich, M. S., and Suresh, D. D., US Patent 4,978,764 (1990); (c) Oshima, K., Kayto, A., Umezawa, T., Kiyono, K., and Sawaki, I., European Patent 529,853 (1992); (d) Kim, Y.-C., Ueda, W., and Moro-oka, Y., *Appl. Catal.* **70**, 189 (1991).
13. Yoon, Y. S., Fujikawa, N., Ueda, W., Moro-oka, Y., and Lee, K. W., *Catal. Today* **24**, 327 (1995).
14. Cavani, F., and Trifiro, F., *Catal. Today* **24**, 307 (1995).
15. Keeling, R. O., *Acta Crystallogr.* **10**, 209 (1957).
16. Smith, G. W., and Ibers, J. A., *Acta Crystallogr.* **19**, 169 (1965).
17. Sleight, A. W., and Chamberland, B. L., *Inorg. Chem.* **8**, 1672 (1968).
18. Young, A. P., and Schwartz, C. M., *Science* **141**, 348 (1963).
19. Wells, A. F., "Structural Inorganic Chemistry," p. 1294. Clarendon Press, Oxford, 1984.
20. Stern, D. L., and Grasselli, R. K., *J. Catal.* **167**, 560 (1997).
21. Callahan, J. L., and Grasselli, R. K., *AIChEJ.* **9**, 755 (1963).
22. Grasselli, R. K., "Ammoxidation: Handbook of Heterogeneous Catalysis" (G. Ertl, H. Knözinger, J. Weitkamp, Eds.). (1997).
23. (a) Grasselli, R. K., Suresh, D. D., and Hardman, H. F., US Patent 4,139,552 (1979); US Patent 4,162,234 (1979); US Patent 4,190,608 (1980); US Patent 4,778,930 (1988); (b) Grasselli, R. K., and Hardman, H. F., US Patent 4,503,001 (1985); (c) Suresh, D. D., Friedrich, M. S., and Seely, M. J., US Patent 5,212,137 (1993).